Tryptophan Rotamer Distributions in Amphipathic Peptides at a Lipid Surface

Andrew H. A. Clayton and William H. Sawyer
The Russell Grimwade School of Biochemistry and Molecular Biology, The University of Melbourne, Parkville, Victoria 3052, Australia

ABSTRACT   The fluorescence decay of tryptophan is a sensitive indicator of its local environment within a peptide or protein. We describe the use of frequency domain fluorescence spectroscopy to determine the conformational and environmental changes associated with the interaction of single tryptophan amphipathic peptides with a phospholipid surface. The five 18-residue peptides studied are based on a class A amphipathic peptide known to associate with lipid bilayers. The peptides contain a single tryptophan located at positions 2, 3, 7, 12, or 14 in the sequence. In aqueous solution, the peptides are unstructured and a triple-exponential function is required to fit the decay data. Association of the peptides with small unilamellar vesicles composed of egg phosphatidylcholine reduces the complexity of the fluorescence decays to a double exponential function, with a reduced dependence of the preexponential amplitude on peptide sequence. The data are interpreted in terms of a rotamer model in which the modality and relative proportions of the lifetime components are related to the population distribution of tryptophan χ_1 rotamers about the C_α-C_β bond. Peptide secondary structure and the disposition of the tryptophan residue relative to the lipid and aqueous phases in the peptide-lipid complex affect the local environment of tryptophan and influence the distribution of side-chain rotamers. The results show that measurement of the temporal decay of tryptophan emission provides a useful adjunct to other biophysical techniques for investigating peptide-lipid and protein-membrane interactions.

INTRODUCTION

The complex fluorescence of tryptophan in polypeptides and proteins has been attributed either to a distribution of conformational states, each with its own lifetime (Rosato et al., 1990), or to the presence of ground state conformers that are quenched to varying degrees by functional groups in the microenvironment surrounding the indole ring (Szabo and Rayner, 1980; Petrich et al., 1983; Dahms and Szabo, 1995). In the latter case, the ground-state conformers have been identified as rotamers of tryptophan that arise from the rotation of the indole ring about the C_α-C_β bond and/or the C_β-C_γ bond, the interconversion between rotamers being slow relative to the fluorescence time scale. Distinct lifetime values for each rotamer arise from quenching interactions between the indole fluorophore and quenching groups in the polypeptide, the quenching efficiency being controlled by the orientation of the groups and the distance dependence of the quenching process. Peptide moieties that can quench tryptophan fluorescence include ionic species (e.g., histidyl, carboxyl, guanidino groups), disulfide bonds, methionyl sulfur, sulfydryl groups, and the carbonyl groups of peptide bonds (Alcala et al., 1987a).

An attractive aspect of the rotamer model is that analysis of tryptophan emission in terms of discrete lifetime components has a clear physical meaning. The preexponential amplitudes are proportional to the relative population of each rotamer present, and the time constants are determined by the local environment of each rotamer. Such correlations are amenable to experimental verification by other methods. Ross et al. (1992) found good agreement between the rotamer populations deduced from NMR experiments and those derived from the preexponential factors of the fluorescence decay. Recently, Dahms et al. (1995) have shown that the fluorescence decay of tryptophan in crystals of erabutoxin is dependent on the rotation of the crystal relative to the polarization direction of the excitation beam, behavior that arises from the selective excitation of certain rotamers within the population of conformers.

The preexponential factors, and by inference the distribution of rotamer forms, may also be influenced by the secondary structure of the protein. Szabo and co-workers (Willis et al., 1994; Dahms et al., 1995) have noted a connection between secondary structure as measured by circular dichroism and the preexponential factors of the fluorescence decay curve of peptides. In protein unfolding experiments, several groups have reported that the time constants of the fluorescence decay are largely insensitive to folding, but that the preexponential factors are more responsive to structural changes (Brown et al., 1994; Szpikowska et al., 1994).

The description of tryptophan emission in terms of rotamer populations raises the interesting question of whether the distribution of rotamer forms can be affected by conformational changes induced by the binding of ligands to peptides or proteins. We examine the question in relation to the binding of 18-residue amphipathic peptides to lipid bilayers, and make use of a series of peptides that have a single tryptophan residue on the hydrophilic or the hydro-

phobic face of the amphipathic helix. The general spectro-scopic characteristics of these peptides, both free in solution and bound to a phospholipid bilayer surface, have been reported previously (Clayton and Sawyer, 1999). The data showed that the peptides, which are unstructured in aqueous solution, associate with the bilayer surface to form an α-helix such that the tryptophan residues located on the hydrophobic face of the α-helix are in the hydrophobic environment provided by the lipid surface, whereas tryptophans located on the hydrophilic face of the helix are directed toward the aqueous phase. The study concludes that the helical axis of these peptides lies approximately parallel to the lipid surface. In this paper we examine the change in the rotamer distribution of the tryptophan residue that results from the association the peptides with a phospholipid surface.

MATERIALS AND METHODS

Materials

Egg yolk phosphatidylcholine was purchased from Lipid Products (Nutfield, U.K.). Peptides with the sequences listed in Table 1 and Fig. 1 were synthesized using automated solid-state synthesis in conjunction with Fmoc chemistry as described previously (Clayton and Sawyer, 1999). Purification was by reverse-phase HPLC, and the purity and identity of the peptides were checked by matrix-assisted laser desorption and ionization time-of-flight mass spectrometry (MALDI-TOF).

Methods

Small unilamellar vesicles were prepared by sonication of a suspension of egg yolk phosphatidylcholine in 10 mM Tris buffer, 150 mM NaCl, pH 7.4, as described by New (1990). Peptide-lipid complexes were prepared by addition of an aqueous suspension of vesicles to a solution containing a known concentration of peptide. The final concentrations of peptide and lipid were 20 μM and 4 mM, respectively, to give a lipid-to-peptide molar ratio of 200:1. Fluorescence intensity and anisotropy titrations showed that under these conditions all the peptide was bound to the lipid surface (results not shown).

Fluorescence lifetimes were measured with a SPEX Fluorolog-τ2 frequency domain spectrofluorometer employing 20–30 frequencies in the range 5–250 MHz. Excitation of tryptophan was accomplished using vertically polarized 295 nm excitation from a 1000 W Hg-Xe lamp (Oriel Model 1909M). An emission polarizer was set at 55° to avoid polarization bias artefacts, and the tryptophan fluorescence was observed through a 335 WD band-pass filter. The cell block was maintained at 20°C with a circulating water bath. Globals Unlimited software (University of Illinois, Urbana-Champaign) was used to fit the frequency domain data to a model involving the sum of discrete exponential lifetime components, or a model describing a distribution of lifetimes. The goodness-of-fit was determined by χ^2 analysis. A comparison of different fluorescence decay models was made by inspection of a χ^2 ratio (χ^2_R) between the model under consideration and a defined model. For the individual free-float sum-of-exponential decay analysis the ratio χ^2_R was that between the free-float parameter model χ^2 and a single exponential decay model χ^2. To assess the penalty associated with linking parameters globally, the global-linked χ^2 for each peptide was divided by the "best fit" sum-of-exponential χ^2.

RESULTS

Steady-state fluorescence spectroscopy

The steady-state fluorescence data of the peptides dissolved in aqueous solution (Tris 10 mM, 150 mM NaCl, pH 7.4) and complexed with phosphatidylcholine small unilamellar vesicles (molar ratio phospholipid/protein, 200:1) are shown in Table 1. The relative quantum yield data were taken from our previous measurements at higher molar ratios of phospholipid/protein (1300:1) (Clayton and Sawyer, 1999). The emission maxima of the peptides in aqueous solution were in the range 350–354 nm, indicating that the tryptophan residue in each peptide was in an aqueous environment. There was no apparent trend in the emission maximum with tryptophan sequence position. In solution, the tryptophan fluorescence quantum yield ratios (relative to trp at pH 7.4) undergo an increase from peptide A to peptide E as the tryptophan is moved toward the C-terminal end of the peptide. In the presence of phosphatidylcholine vesicles, the emission maxima of peptides A, B, C, and E were blue-shifted to wavelengths characteristic of tryptophan in an environment of low dielectric constant. The tryptophan fluorescence quantum yields undergo an increase in peptides A, B, and C, a decrease in peptide E, and essentially no change in peptide D in the peptide-lipid complexes. The emission maximum of peptide D indicates that its tryptophan residue is exposed to an aqueous environment. This pattern is consistent with previous results showing that the peptides associate with the vesicles with the α-helical axis parallel to the bilayer surface according to the helical wheel representation depicted in Fig. 1 (Clayton and Sawyer, 1999).

### Time-resolved fluorescence

Discrete decay components

The frequency domain data for the peptides in solution were fitted to a discrete decay model involving the sum of up to

TABLE 1 Sequence of amphipathic peptides, wavelengths of their emission maxima (λ), and quantum yield ratios (R, relative to tryptophan at pH 7.4) in solution and when complexed to unilamellar bilayer vesicles composed of egg phosphatidylcholine

Peptide	Sequence	Steady-State Fluorescence Data			
		$\lambda_{\text{solution}}$	λ_{bilayer}	R_{solution}	R_{bilayer}
18A-2	DWLKAFYDKVAEKLKEAF	353	341	0.51	0.68
18B-3	DRWKAFYDKVAEKLKEAF	353	340	0.74	0.95
18C-7	DRLKAFWDKVAEKLKEAF	353	339	0.85	1.17
18D-12	DRLKAFYDKVAWKLKEAF	354	354	0.84	0.85
18E-14	DRLKAFYDKVAEKWKEAF	350	344	1.04	0.85

FIGURE 1 Helical wheel representation of 18-residue amphipathic peptides. The figures in bold refer to the positions of tryptophan substitution in peptides A–E. The solid line represents the putative boundary between the hydrophilic and hydrophobic faces of the α-helix.

	Peptide
2	
DWLKAF<u>Y</u>DKVAEKLKEAF	A
3	
DRWKAF<u>Y</u>DKVAEKLKEAF	B
7	
DRLKAFWDKVAEKLKEAF	C
12	
DRLKAF<u>Y</u>DKVAWKLKEAF	D
14	
DRLKAF<u>Y</u>DKVAEKWKEAF	E
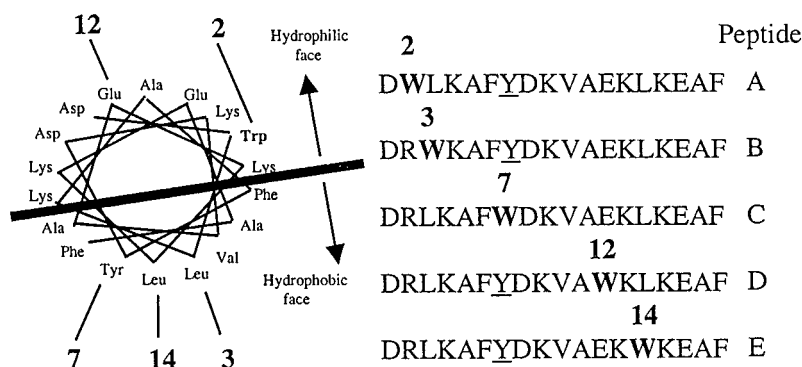
three exponential terms.

$$I(t) = A_1\exp(-t/\tau_1) + A_2\exp(-t/\tau_2) + A_3\exp(-t/\tau_3) \quad (1)$$

where τ_1, τ_2, and τ_3 are the time constants of the decay and A_1, A_2, and A_3 are the corresponding preexponential population amplitudes.

The data for the peptides in solution were fitted in two stages. In the first stage, the fluorescence decay of each peptide was analyzed separately and the preexponential factors and lifetimes were allowed to float in the fitting procedure. The data could be described by three similar time constants and associated preexponential amplitudes, the average values being 0.8 ns, 3.0 ns, and 6.0 ns, and 35%, 51%, and 14%, respectively (Table 2). We questioned whether the data for the peptides in solution could be described equally well by a model where the time constants were common to all peptides and the preexponential amplitudes allowed to vary with each peptide. In the second stage, the data for the five peptides were analyzed globally but with the three time constants common to all five peptides, and therefore linked in the analysis. The preexponential factors were allowed to float. This global approach required only 13 independent floating parameters, compared with 25 for the single curve analysis of the entire data set. The ratio of the global chi-squared to that of the free-parameter-float chi-squared

was used to assess the fitting penalty in linking the parameters and was in the range 1.2–1.6 (Table 3). Thus, the data for the five peptides could be fitted globally, with sequence-independent decay times, which were linked in the analysis, and sequence-dependent preexponential amplitudes. A typical global fit of the experimental data is presented in Fig. 2 and the results are summarized in Table 3.

For peptides A–E in aqueous solution, the preexponential amplitudes were unique for each peptide and exhibited an approximate monotonic trend with tryptophan sequence position from peptide A to peptide E (Table 3). In progressing from position 2 to position 14, the magnitude of the intermediate amplitude decreased by 0.23 and the amplitude associated with the long time constant increased by 0.41 (Table 3), resulting in a gradual increase in the average lifetime as the tryptophan moved progressively along the sequence from position 2 to position 14.

An alternative model involving a common set of linked preexponential population amplitudes and floated time constants was also analyzed but did not produce a one-to-one correspondence between lifetime category (i.e., "short," "medium," or "long") and preexponential amplitude.

Analysis of the individual peptide-lipid complexes revealed that only two exponential terms were required to adequately fit the data for all peptides (Table 2, Fig. 3).

TABLE 2 Lifetimes (τ_i), preexponential population amplitudes (A_i), and average population-weighted lifetimes ($\langle\tau\rangle$) for 18-residue amphipathic peptides in solution ($-v$) and bound to unilamellar bilayer vesicles ($+v$)

Peptide	Environment	τ_1 (ns)	τ_2 (ns)	τ_3 (ns)	A_1 (%)	A_2 (%)	A_3 (%)	$\langle\tau\rangle$	χ^2_R
18A-2	$-v$	0.200	2.091	4.870	38	54	8	1.59	0.1
	$+v$	—	2.582	6.160	—	70	30	3.65	0.4
18B-3	$-v$	0.174	1.995	4.144	30	40	30	2.09	<0.1
	$+v$	—	2.640	6.973	—	72	28	3.72	0.2
18C-7	$-v$	1.266	3.365	5.765	35	49	16	3.00	<0.1
	$+v$	—	2.270	6.454	—	64	36	3.78	0.3
18D-12	$-v$	1.137	3.698	8.964	39	59	3	2.64	<0.1
	$+v$	—	3.167	9.174	—	75	25	4.67	0.2
18E-14	$-v$	1.251	4.010	6.123	31	53	16	3.50	0.1
	$+v$	—	2.494	6.000	—	71	29	3.51	0.3
Average	$-v$	0.805	3.030	5.970	35	51	14	2.56	
	$+v$	—	2.691	6.952	—	70	30	3.90	

The chi-squared ratio (χ^2_R) is defined as the ratio of the chi-squared from the multi-exponential fit to that of the chi-squared from a single exponential fit.

TABLE 3 Global-linked lifetimes (τ_i), preexponential population factors (A_i), and average population-weighted lifetime ($\langle\tau\rangle$) for 18-residue amphipathic peptides in solution ($-v$) and bound to unilamellar bilayer vesicles ($+v$)

Peptide	Environment	τ_1 (ns)	τ_2 (ns)	τ_3 (ns)	A_1 (%)	A_2 (%)	A_3 (%)	$\langle\tau\rangle$	χ^2_R
						Lifetime Data			
18A-2	$-v$	0.623	2.416	5.114	34	60	6	1.97	1.4
	$+v$	—	2.929	7.917	—	85	15	3.68	1.2
18B-3	$-v$	0.623	2.416	5.114	21	62	17	2.50	1.6
	$+v$	—	2.929	7.917	—	80	20	3.93	1.1
18C-7	$-v$	0.623	2.416	5.114	18	53	29	2.88	1.2
	$+v$	—	2.929	7.917	—	79	21	3.98	1.1
18D-12	$-v$	0.623	2.416	5.114	22	51	27	2.75	1.2
	$+v$	—	2.929	7.917	—	65	35	4.68	1.2
18E-14	$-v$	0.623	2.416	5.114	17	37	47	3.40	1.2
	$+v$	—	2.929	7.917	—	86	14	3.63	1.1
Average	$-v$	0.623	2.416	5.114	22	53	25	2.70	
	$+v$	—	2.929	7.917	—	79	21	3.98	

The chi-squared ratio (χ^2_R) is the ratio between the linked-lifetime analysis chi-squared and the unlinked-lifetime analysis chi-squared.

Addition of a third component did not improve the goodness-of-fit as judged by χ^2 analysis. A discrete subnanosecond lifetime of ~50 ps was included in the fitting function to account for vesicle scatter. The fractional contribution of this scatter component (0.05) agreed with that determined by steady-state measurements. A free-floating-parameter analysis revealed two time constants: a medium lifetime in the range 2.3–3.2 ns and a long lifetime of 5.9–9.1 ns (Table 2). These time constants appear to be nearly independent of peptide sequence for peptides A, B, C, and E, but somewhat longer for peptide D. As for the peptides in solution, a global analysis linking the time constants was performed for the peptide-lipid complexes. The low values of the chi-squared ratios between global and individual fits (1.1–1.2) and a comparison between the average lifetimes from the two fitting schemes indicated that a global approach provided an equivalent description of the emission decay for these peptide-lipid complexes (Tables 2 and 3). A linked-lifetime global analysis revealed two time constants: a medium lifetime of 2.9 ns and a long lifetime of 7.9 ns (Table 3, Fig. 3). The floated preexponential amplitudes were found to be unique for each tryptophan position in the

peptide. For the four peptides with fluorescence maxima < 350 nm (peptides A, B, C, and E) the standard deviation in the preexponential amplitude of the medium time constant was 3%. The preexponential amplitudes associated with tryptophan at position 12 (peptide D) were significantly different from those of the other peptides. A model involving common linked preexponential amplitudes (and floated time constants) was also analyzed but gave poorer fits than the linked-lifetime analysis ($\chi^2_R > 3$).

Rotation about the C_α-C_β bond of tryptophan gives rise to the three rotamer forms (t, $g+$, $g-$) depicted as the Newman projections in Fig. 3. The distribution of these rotamer forms in native proteins has been determined from x-ray crystallographic data by McGregor et al. (1987), and by Shrauber et al. (1993), and is sensitive to the secondary structure of the polypeptide main chain. The database of Shrauber includes data from proteins containing side-chain rotamers under steric strain, a situation that is not expected to occur in small peptides (Benedetti et al., 1983). There-
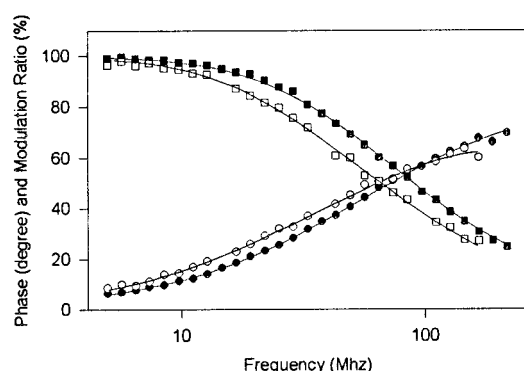

FIGURE 2 Multifrequency measurement of the phase (*circles*) and modulation (*squares*) of the tryptophan decay for peptide B in aqueous solution (*filled symbols*), and for the peptide B-bilayer complex (*open symbols*). The solid lines represent the fits of the data reported in Table 3.
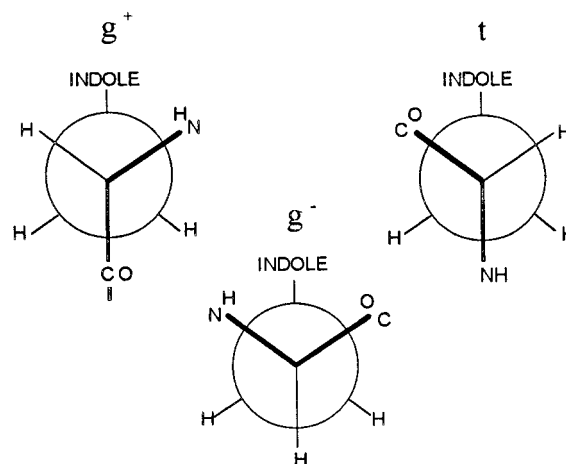

FIGURE 3 Tryptophan χ_1 rotamers of the indole side chain of tryptophan. The Newman projections indicate the rotation of the indole group about the C_α-C_β bond.

fore, the earlier data of McGregor et al. (1987) are presented here (Table 1 from the McGregor reference). Fig. 4 *a* summarizes data pertaining to the tryptophan rotamer distributions in α-helical regions (*unshaded bars*) and unordered regions (*shaded bars*) of globular proteins. Fig. 4 *b* shows the average values of the tryptophan fluorescence decay preexponential amplitudes for the peptides in the presence (*unshaded bars*) and absence (*shaded bars*) of lipid vesicles from the lifetime-linked global analysis. Of particular note is the similarity of the average preexponential amplitudes for the peptides in solution with rotamer distributions of tryptophan residues in unordered regions of globular proteins. Likewise, there is a striking similarity between the average preexponential factors for the peptide-lipid complexes and the rotamer distributions for tryptophan residues found with α-helical regions of globular proteins.

Lifetime distribution analysis

Complex decays of fluorescence can also be analyzed in terms of a lifetime distribution model. Unimodal Gaussian and Lorentzian lifetime distributions could describe the emission decays of the peptides in solution and when associated with lipid vesicles. A discrete subnanosecond lifetime term was included in the fitting function for the peptide-lipid complexes to account for vesicle scatter. There was no correlation between individual distribution width,

tryptophan sequence position, or environment (buffer or lipid) for these unimodal distributions (data not shown).

DISCUSSION

Tryptophan rotamer distributions for peptides in aqueous solution

Complex fluorescence decay kinetics is a general feature of many tryptophan containing peptides and proteins and has been the subject of much debate. The triphasic decay observed for peptides A–D in solution could be due to several factors: 1) to local interactions about the indole fluorophore, 2) to interconversion between conformational isomers of the peptide during the excited state lifetime, or 3) to the presence of tryptophan rotamer populations that do not interconvert during the excited state lifetime. If specific or local interactions of the indole side chain were the dominant determinant of the lifetime heterogeneity, then the lifetimes would depend on the position of the tryptophan residue in the sequence since the types of side chains that flank the tryptophan are different in peptides A–E. The finding that the lifetimes are *largely independent* of the tryptophan position suggests that side-chain interactions are not the major cause of the triphasic decay kinetics. However, minor variations in the individual time constants with sequence position may be affected by local interactions with proximal amino acid side chains and the solvent. An alternative model involves interconversion between at least three different conformational states during the excited state lifetime. In this model, changes in the preexponential factors and/or lifetimes of the tryptophans in different positions result from changes in interconversion rates between excited-state environments (Alcala et al., 1987a). As such we cannot distinguish between models 2) and 3) from the individual decay curve analysis alone because both slight variations in time-constant and/or preexponential amplitude are observed. However, as we shall see below, a comparison of x-ray population data on proteins and peptides with the preexponential amplitudes of the peptides A–E as a whole indicated a correlation between the ground state rotamer distribution in proteins and the preexponential factors resolved in the fluorescence decays of peptides A–E in solution. We therefore propose that the observed kinetics result mainly, but by no means exclusively, from three rotamer populations of the indole side chain that are stable on the fluorescence time scale, with the proportion of each rotamer being moderately dependent on the tryptophan position in the sequence.

It is likely that the influence of sequence position on the rotamer distribution is an effect that is secondary to an intrinsic preference of the indole side chain for certain rotamer forms. The use of an average rotamer distribution for the five peptides would therefore tend to average out the effects of sequence position, resulting in a distribution that reflected the intrinsic rotamer distribution. The following evidence supports this interpretation:
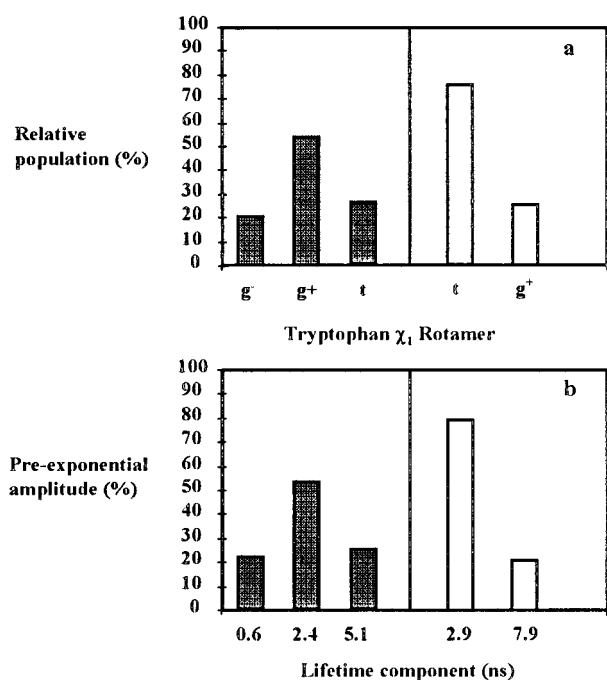

FIGURE 4 Comparison of the average distribution of rotamers determined from the preexponential amplitudes of the fluorescence decay for peptides A–E (lifetime-linked global analysis) with the average distributions of *t, g+,* and *g−* rotamers derived from x-ray crystallographic data of proteins (McGregor et al., 1987). (*a*) Shaded bars, disordered; unshaded bars, α-helix). (*b*) Shaded bars, buffer; unshaded bars, lipid).

1. The average preexponential factors corresponding to the short, medium, and long lifetime components of peptides A–E in solution [A_{1-3} = 22 ± 7%, 53 ± 10%, 25 ± 15% (±SD)] (lifetime-linked analysis), [A_{1-3} = 35 ± 7%, 51 ± 10%, 14 ± 15% (±SD)] (unlinked analysis) are similar to those observed for denatured-erabatoxin peptides (A_{1-3} = 28%, 45%, 27%) (Dahms et al., 1995) and for nine denatured single tryptophan proteins (A_{1-3} = 23%, 47%, 30%) (Swaminathan et al., 1994).

2. The average preexponential factors of the three lifetime forms of peptides A–E (A_{1-3} = 22%, 53%, 25%) match closely to the average χ_1 rotamer distributions of tryptophan residues located in unstructured (non-α/non-β) regions of native proteins as determined by x-ray crystallography (A_{1-3} = 20%, 54%, 26%, McGregor et al., 1987; A_{1-3} = 18%, 61%, 22%, Shrauber et al., 1993). The correlation between the x-ray data and the excited-state amplitudes provides additional evidence that the rotamers are not interconverting on the fluorescence time scale.

We therefore suggest that for peptides in an unordered conformation in solution the preexponential factors are determined by an intrinsic preference for certain rotamer forms and that the influence of sequence position is a secondary effect that is overlaid on a primary effect determined by the unordered conformation of the peptide.

Tryptophan rotamer distributions for peptides bound to phospholipid bilayers

The interaction of the peptide with a lipid surface reduces the number of lifetime components, and by inference the number of rotamer forms, from three to two (Tables 2 and 3). Although sequence dependence of the preexponential factors is again observed, it is apparent that the medium lifetime component is favored with 64–86% of the decay attributed to this form, compared to 37–60% for the peptides in solution. The lifetimes of the two components are increased over the comparable lifetimes for the peptides in solution, indicating that the local environment of each tryptophan is changed on binding to the lipid surface. One possible cause for the reduced number of decay components relates to the α-helix conformation adopted by the peptides on the bilayer surface. In terms of rotamer conformations, the significance of the α-helix is that the (i-3)th main-chain carbonyl sterically interferes with the tryptophan $g-$ rotamer, resulting in a reduction in the population of this rotamer form (McGregor et al., 1987; Shrauber et al., 1993). An alternative explanation is that a third rotamer is populated but is strongly quenched by interaction with the main-chain peptide carbonyl or with a proximal side chain, resulting in a short-lifetime undetected species. A small population of $g-$ rotamers with χ_2 angles outside of 90° has been observed for tryptophans in α-helical regions of proteins (Shrauber et al., 1993). Knutson and co-workers (Chen et al., 1991) have noted the importance of rotamers involved in strong indole-carbonyl interactions and exhibiting short, unresolvable lifetimes (termed quasi-static quenching) in dipeptides. The disproportionate increase in average lifetime to that of the relative fluorescence quantum yield in the peptide-lipid complexes as compared with that for the peptides in aqueous solution may be partly attributed to this effect (Tables 1–3). It is unlikely that our instrumentation could resolve a short subnanosecond lifetime above a short-lived scatter contribution. A third possibility is that some environmental averaging (e.g., between two or more rotamers) occurs via dynamic excited-state interconversion on the subnanosecond time scale. However, this possibility is unlikely since anisotropy measurements show that the indole ring mobility is decreased on binding to the lipid surface (Clayton and Sawyer, 1999).

Additional evidence that the rotamer preference is determined, at least in part, by the α-helical conformation of the peptide comes from two quarters. First, using pulsed time-domain techniques, Szabo and colleagues observed that the preexponential factors were dependent on the secondary structure proximal to the indole fluorophore as measured for folded and unfolded peptides with different degrees of α-helical or β-sheet structure (Willis et al., 1994; Dahms et al., 1995). They suggested that the different lifetimes observed were characteristic of different tryptophan χ_1 side-chain rotamers and that the relative proportion of rotamers was affected by the local secondary structure. Second, surveys of x-ray crystallographic structures of proteins also suggest that the tryptophan rotamer distributions in globular proteins are strongly influenced by the secondary structure adopted by the main chain of the polypeptide local to the indole fluorophore, as defined by the ϕ and ψ angles (Janin et al., 1978; McGregor et al., 1987; Shrauber et al., 1993). The influence of the α-helix on rotamer distribution receives strong support from detailed analysis of x-ray crystallographic data of proteins. Tryptophan rotamers are found in two major χ_1 rotamer forms in α-helices, with a distribution of 77%/23% for ideal α-helices (Trp χ_2 angles close to the preferred value of 90°), 65%/35% for deformed α-helices (Shrauber et al., 1993), and 75%/25% (McGregor et al., 1987) for tryptophans near the middle of the α-helices. These values compare favorably with the average distributions of 79%/21% (global analysis) and 70%/30% (unlinked analysis) found for our helical peptide-lipid complexes. Such agreement is not found for χ_1 tryptophan rotamer distributions pertaining to nonhelical regions or to tryptophans near the ends of helices in globular proteins (McGregor et al., 1987). We note that inclusion of trp rotamers with χ_2 angles outside the preferred value of 90° produces a trimodal distribution of Trp χ_1 rotamers with relative frequencies of 14%/63%/22% in α-helical regions of proteins (Shrauber et al., 1993).

The availability of the five single-tryptophan peptide analogs allows one to probe in more detail the consequences of the peptide-lipid interaction at particular tryptophan positions. An important observation is that the average lifetime is a function of tryptophan sequence position for the

peptides in solution, but is also determined by the helical face in which the tryptophan is located when the peptide is bound to lipid. Thus, according to the linked-lifetime analysis (Table 3) the preexponential factors for peptide D in the lipid-peptide complex yield proportions of 65% and 35% for the medium- and long-lifetime components, while for the tryptophans at other positions the corresponding values are in the ranges 80–85% and 15–20%. One possibility is that location of the tryptophan at position 12 could potentially lead to local helix deformation via disruption of the lysine-glutamate salt link, and by inference a change in rotamer population. However, our circular dichroism measurements could not detect a reduced overall helicy for peptide D as compared with the other positions (Clayton and Sawyer, 1999). From Table 2 the influence on average lifetime can be alternatively ascribed to the longer lifetime component of 9 ns at position 12 as compared with the lower values in the range 6–7 ns at the other positions. Helical wheel representations show that the tryptophan at position 12 in peptide D is located in the middle of the polar face of the helix, while the other positions are either on the nonpolar of face of the helix (peptides B, C, E) or close to the peptide-polar/nonpolar interface (peptide A). We have shown previously that the tryptophan located at position 12 of peptide D is exposed to the aqueous phase while the tryptophans at the other positions are embedded in or face the lipid phase (Clayton and Sawyer, 1999). Thus, in addition to secondary structure, there appear to be local factors related to the orientation of the helix on the lipid surface that influence the distribution and/or environment of different rotamer forms.

Perturbation of rotamer distributions due to the position of a tryptophan residue in a polypeptide has been observed previously. On the basis of crystallographic data, Janin et al. (1978) observed that the χ_1 side-chain rotamer distributions of exposed tryptophan residues in globular proteins are slightly different from those for buried residues. The less populated rotamer is decreased in frequency in the buried state as compared with the exposed state. This is consistent with our observation that the preexponential amplitude of the less populated lifetime is decreased in peptides A, B, C, and E where the tryptophan faces the lipid phase compared with the tryptophan in peptide D, which is exposed to the aqueous environment (Table 3). Such agreement is not observed from the unlinked analysis data set, Table 2. Additional evidence comes from studies of indole-containing compounds in lipids. Chattopadhyay and co-workers (1997) reported double exponential fluorescence kinetics for tryptophan octyl ester embedded in lipid bilayers, and attributed the prevalence of one short decay component to a restriction of tryptophan rotamers caused by specific tryptophan-lipid interactions. Hydrogen bonding interactions of the indole ring of the tryptophan with suitable acceptors in the membrane, either bound water molecules or lipid carbonyls, was a possible cause of the restriction of the tryptophans in the gramicidin ion channel (Mukherjee and Chattopadhyay, 1994), and could in principle contribute to

the rotamer distribution in the present peptides. Another possibility is dipole-dipole interactions between the lipid and tryptophan dipole moments (Wimley and White, 1993). Tryptophans oriented near the interface, which is an anisotropic and motionally restricted region, might also be expected to have less energetically accessible configurations than those facing the aqueous phase. These interactions would be optimized for tryptophan residues located near the interface/headgroup region and may partly explain the difference in emission decay between peptides A/B/C/E and peptide D in the lipid-peptide complexes.

Interactions at the primary structure level may also affect the environment of the different tryptophan rotamer forms, and by inference the individual time constants. In an α-helix the most important side-chain interactions will be between residues flanking at the $i \pm 3$ and $i \pm 4$ positions. Barkley and co-workers (Yu et al., 1995) have observed an increase in indole conformer lifetime due to interactions with proximal charged amino groups (3–5 Å), which decrease solvent (water) quenching rates. This may partly explain why the tryptophan at position 12 in peptide D, which is flanked by two lysines, has a larger average lifetime than at the other positions, which contain one (peptide C) or no (peptides A, B, and E) flanking lysines in the $i \pm 3$ and $i \pm 4$ positions. However, this interpretation assumes that the inherent exposure of the tryptophan residue to the aqueous phase is the same for all peptides; this is certainly not the case for the peptide-lipid complexes. Moreover, as is implicit in the global analysis results, local environment effects (as reflected in linked-rotamer population analysis) appear to be less important than rotamer population effects (from linked lifetime analysis) in accounting for the fluorescence decay differences between the peptide-lipid complexes.

An alternative interpretation of complex decay kinetics is in terms of a distribution of lifetimes rather than the sum of exponential decays. We have modeled the present peptide fluorescence decay data according to unimodal Gaussian and Lorentzian lifetime distributions and found that the centers of the lifetime distributions are similar to the intensity-weighted average lifetimes obtained from the discrete sum-of-exponentials model. However, we could find no correlation between individual distribution width, tryptophan sequence position, or environment (buffer or lipid) for these unimodal distributions (data not shown). We also modeled the data using the asymmetric distribution function employed by Alcala and co-workers to model protein fluorescence (Alcala et al., 1987a,b). This model allows for an asymmetric distribution of lifetimes and is a physical model that assumes that the indole ring moves in a single potential well with a well-width given by a density-of- states parameter (reflecting indole flexibility or range of environment) and a potential-well asymmetry parameter (bounded by a minimum lifetime and a maximum lifetime). Global linkage of the density-of-states parameter gave acceptable fits for the emission of the peptide-lipid complexes. However, use of this more complex mathematical function did not lead to improvement in the quality of the fit compared to the

discrete lifetime model. A correlation was observed between the derived asymmetry parameter and the tryptophan position in the α-helix. In terms of the single potential well model, the derived parameters imply that the indole ring potential energy surface becomes differently distorted depending on whether the tryptophan residue is facing the lipid or the aqueous phase. Such perturbation to the potential well would alter the relative populations of different rotamers/conformational states, a result that is in qualitative accord with our conclusions based on the discrete model involving rotamer distributions.

To conclude, both sequence and conformational effects seem to determine the distribution and environment of tryptophan rotamers when an amphipathic peptide binds to a lipid surface. For the unordered peptides in solution and for the α-helical peptide-lipid complexes, the distribution of rotamer types deduced from the average preexponential amplitudes agrees with the distribution apparent in the x-ray crystal structures of globular proteins. The fluorescence decay of the peptide-phospholipid complexes is determined not only by the adoption of an α-helical conformation but also by whether the tryptophan residue faces the lipid or the aqueous phase. The results indicate that the correlation between the preexponential amplitudes and secondary structure proposed by Willis and Szabo (1992) would appear to be obeyed for peptide-lipid complexes with the additional caveat that the rotamer distribution and environment may be perturbed by local interactions dependent on amino acid sequence and the exposure of the tryptophan within the macromolecule or molecular complex.

REFERENCES

Alcala, J. R., E. Gratton, and F. G. Prendergast. 1987a. Interpretation of fluorescence decays in proteins using continuous lifetime distributions. *Biophys. J.* 51:925–936.

Alcala, J. R., E. Gratton, and F. G. Prendergast. 1987b. Fluorescence lifetime distributions in proteins. *Biophys. J.* 51:597–604.

Benedetti, E., G. Morelli, G. Nemethy, and H. A. Sheraga. 1983. Statistical and energetic analysis of side-chain conformations in oligopeptides. *Int. J. Peptide Protein Res.* 22:1–15.

Brown, M. P., N. Shaikh, M. Brenowitz, and L. Brand. 1994. The allosteric interaction between D-galactose and the *Escherichia coli* galactose repressor protein. *J. Biol. Chem.* 269:12600–12605.

Chattopadhyay, A., R. Mukherjee, R. Rukmini, J. S. Rawat, and S. Sudha. 1997. Ionization, partitioning, and dynamics of tryptophan octyl ester: implications for membrane-bound tryptophan residues. *Biophys. J.* 73:839–849.

Chen, R. F., J. R. Knutson, H. Ziffer, and D. Porter. 1991. Fluorescence of tryptophan dipeptides: correlations with the rotamer model. *Biochemistry*. 30:5184–5195.

Clayton, A. H. A., and W. H. Sawyer. 1999. The structure and orientation of class A amphipathic peptides on a phospholipid bilayer surface. *Eur. Biophys. J.* 28:133–141.

Dahms, T. E. S., and A. G. Szabo. 1995. Probing local secondary structure by fluorescence: time-resolved and circular dichroism studies of highly purified neurotoxins. *Biophys. J.* 69:569–576.

Dahms, T. E. S., K. J. Willis, and A. G. Szabo. 1995. Conformational heterogeneity of tryptophan in a protein crystal. *J. Am. Chem. Soc.* 117:2321–2326.

Janin, J., S. Wodak, M. Levitt, and B. Maigrett. 1978. Conformation of amino acid side-chains in proteins. *J. Mol. Biol.* 125:357–386.

McGregor, M. J., S. A. Islam, and M. J. E. Sternberg. 1987. Analysis of the relationship between side-chain conformation, and secondary structure in globular proteins. *J. Mol. Biol.* 198:295–310.

Mukherjee, S., and A. Chattopadhyay. 1994. Motionally restricted tryptophan environment at the peptide-lipid interface of gramicidin channels. *Biochemistry*. 33:5089–5097.

New, R. R. C. 1990. Preparation of liposomes. *In* Liposomes: A Practical Approach, IRL Press, Oxford, U.K., 1–33.

Petrich, J. W., M. C. Chang, D. B. Mcdonald, and G. R. Fleming. 1983. On the origin of nonexponential fluorescence decay in tryptophan and its derivatives. *J. Am. Chem. Soc.* 105:3824–3832.

Rosato, N., E. Gratton, G. Mei, and A. Finazzi-Agro. 1990. Fluorescence lifetime distributions in human superoxide dismutase. Effect of temperature and denaturation. *Biophys. J.* 58:817–822.

Ross, J. B. A., H. R. Wyssbrod, R. A. Porter, G. P. Schwartz, C. A. Michaels, and W. R. Laws. 1992. Correlation of tryptophan intensity decay parameters with ^{1}H NMR-determined rotamer conformer: [trp[2]] oxytocin. *Biochemistry*. 31:1585–1594.

Shrauber, H., F. Eisenhaber, and P. Argos. 1993. Rotamers: to be or not to be? An analysis of amino-acid side-chain conformations in globular proteins. *J. Mol. Biol.* 230:592–612.

Swaminathan, R., G. Krishnamoorthy, and N. Periasamy. 1994. Similarity of fluorescence lifetime distributions for single tryptophan proteins in the random coil state. *Biophys. J.* 67:2013–2023.

Szabo, A. G., and D. M. Rayner. 1980. Fluorescence decay of tryptophan conformers in aqueous solution. *J. Am. Chem. Soc.* 102:554–563.

Szpikowska, B. K., J. M. Beecham, M. A. Sherman, and M. T. Mas. 1994. Equilibrium unfolding of yeast phosphoglycerate kinase, and its mutants lacking one or both native tryptophans: a circular dichroism, and steady-state, and time-resolved fluorescence study. *Biochemistry*. 33:2217–2225.

Willis, K. J., W. Neugebawer, M. Sikorska, and A. G. Szabo. 1994. Probing α-helical secondary structure at a specific site in model peptides via restriction of tryptophan side-chain rotamer conformation. *Biophys. J.* 66:1623–1630.

Willis, K. J., and A. G. Szabo. 1992. Conformation of parathyroid hormone: time-resolved fluorescence studies. *Biochemistry*. 31:8924–8931.

Wimley, W. C., and S. H. White. 1993. Membrane partitioning: distinguishing bilayer effects from the hydrophobic effect. *Biochemistry*. 32:6307–6312.

Yu, H. T., M. A. Vela, F. R. Fronczek, M. L. McLauglin, and M. D. Barkley. 1995. Microenvironmental effects on the solvent quenching rate in constrained tryptophan derivatives. *J. Am. Chem. Soc.* 117:348–357.